Carbohydrate Polymers 79 (2010) 318–324

Contents lists available at ScienceDirect

Carbohydrate Polymers

journal homepage: www.elsevier.com/locate/carbpol

Electrorheological behavior of biodegradable modified corn starch/corn oil suspensions

Mustafa Yavuz [a,*], Tahir Tilki [a], Cigdem Karabacak [a], Ozlem Erol [b], H. Ibrahim Unal [b], Mehmet Uluturk [a], Mehmet Cabuk [c]

[a] *Suleyman Demirel University, Faculty of Sciences and Arts, Department of Chemistry, Isparta, Turkey*
[b] *Gazi University, Faculty of Sciences, Department of Chemistry, Rheology Group, Ankara, Turkey*
[c] *Mus Alparslan University, Faculty of Sciences and Arts, Department of Chemistry, Mus, Turkey*

ARTICLE INFO

Article history:
Received 24 February 2009
Received in revised form 21 July 2009
Accepted 6 August 2009
Available online 12 August 2009

Keywords:
Modified starch
Anhydrous ER fluids
Biodegradable polymer
Creep behavior

ABSTRACT

In this study, an electrorheological (ER) effect of the suspensions containing both native starch (S) and modified starch (MS) particles in corn oil (CO) under various externally applied electric field strengths (*E*) are reported. To prepare an ER active material, biodegradable starch was partially hydrolyzed and converted to its Li-salt. Both biopolymers (S and MS) were characterized by FT-IR, ^{1}H and ^{13}C NMR, SEM, energy dispersive spectroscopy (EDS), TGA and conductivity measurements. Suspensions of S and MS particles were prepared in CO at concentrations ranging from 5% to 40% by mass. Effects of various parameters such as sedimentation stability, particle size, dispersed particle concentration, electric field strength, shear rate, frequency and temperature onto ER activity of suspensions were investigated. Further, creep behaviors of S/CO and MS/CO suspensions were also investigated.

1. Introduction

Starch is the only qualitatively important digestible polysaccharide and has been regarded as nutritionally superior to low molecular weight carbohydrate or sugars. The modern food processing industries are increasingly dependent on the use of both native and modified starches (and gums as well) for manufacture of various fabricated food products. Clarity varies considerably with the sources of starch and can be altered by chemical modification. A number of modifications/derivatizations via chemical treatments are reported in the literature for various purposes (Ogungbenle, 2007).

Rheological properties of ER fluids can be dramatically changed by an externally imposed electric field (*E*). Commonly, they are composed of a suspension of polarizable solid particles dispersed in an insulating liquid. When an *E* is imposed, the rheological properties of the fluid vary, showing a characteristic fibrillation; the strings of the particles are oriented along the direction of *E*. This structure is known to be induced by a mismatch of the dielectric constants of the suspended particles and the insulating oil (Parthasarathy & Klingenberg, 1996). Furthermore, this may not be the only mechanism, and the ER phenomenon can also be explained by the conductivity model (Gonon, Foulc, & Atten, 2001). The ER fluids can solidify in the order of milliseconds, and can also fluidize under applied deformation which destroys the chain structure formed by the electric field induced particles. Because of the controllable rheological properties, ER fluids can potentially be used as a smart material for active devices including actuators, torque transducers and dampers (Shimada, Nishida, & Fujita, 2001), which transform electrical energy to mechanical energy (Kim, Cho, Choi, Lee, & Choi, 2002).

ER fluids are divided into two categories: one is called dry-base ER system (or anhydrous, which shows ER activity without adding any polar promoter) (An, Liu, & Shaw, 2002); the other one is called wet-base ER systems (or hydrous, which needs a polar promoter to be added to show ER activity) (Okamura et al., 2002). Anhydrous ER systems have attracted more attention due to their physicochemical characteristics as compared to the hydrous systems. Many semiconducting polymers, (Hao, Xu, & Xu, 1997) biopolymers and polymer/clay nanocomposites (Kim, Choi, & Jhon, 2000; Kim, Noh, Choi, Lee, & Jhon, 2000) are known as dry-base smart ER materials when dispersed in insulating oil. Due to the importance of biopolymers in ER applications, modified cellulose and chitosan have also been examined as anhydrous ER materials (Hong, Sung, & Choi, 2009; Park, Sung, Kim, Choi, & Jhon, 2004).

In fact, the high performance ER materials are closely related to their molecular structures. With the development of ER materials, it is clear that those materials possess either branched polar groups such as amine (–NH$_2$), hydroxyl (–OH), and carboxyl (–COOH) or semiconducting repeated units. The polar groups may affect the ER behavior by playing the role of an electronic donor under the

---

* Corresponding author. Tel.: +90 246 211 40 83; fax: +90 246 237 11 06.
E-mail addresses: yavuz@fef.sdu.edu.tr, efeym@yahoo.com (M. Yavuz).

0144-8617/$ - see front matter © 2009 Elsevier Ltd. All rights reserved.
doi:10.1016/j.carbpol.2009.08.008

imposed *E*. (Kim, Kim, Jang, Choi, & Jhon, 2001). Therefore, the chemical structure of the materials is a primary factor in ER performance. (Gao & Zhao, 2004).

In this study, we have investigated the ER properties of biodegradable native starch and modified starch. Before the ER measurements to be carried out, particle sizes, conductivities and sedimentation stabilities of the suspensions were determined. Both materials were characterized by a set of techniques namely: FT-IR, ^{1}H NMR, ^{13}C NMR, TGA, SEM and EDS. The effects of dispersed particle concentration, electric field strength, shear rate, frequency and temperature onto ER performance of the materials were searched. Creep behaviors of the suspensions were investigated.

2. Experimental

2.1. Materials

All the chemicals used were Aldrich products with analytical grade and used as received. The host oil employed was food-grade corn oil produced by Luna and had the following physical properties at 25 °C: density (ρ) = 0.936 g/cm^3, viscosity (η) = 45 mPa s, dielectric constant (ε = 3.34 and conductivity ($\sigma = 4 \times 10^{-11}$ S/m. The starch (S) was (used as dispersed phase) produced by Acros Organics products.

2.2. Modification of the starch

Suspensions of the air-dried corn starch (50 g) in distilled water (500 mL) were supplemented with ammonium vanadate (NH_4VO_3). A marine blue color was appeared. The pH of each suspension was adjusted to 9.0 by adding 10% $NaOH_{(aq)}$. Each suspension was continuously stirred for 48 h at a constant temperature of 35–40 °C, under atmospheric conditions. After the reaction was completed, its color turned to yellowish. The reaction mixture was filtered through a sintered glass and the filtrate washed with cold water to remove any impurities present. The products were dried in desiccators over molecular sieves. The dried products were dispersed in 0.1 M $LiOH_{(aq)}$ and the Li-salt of partially modified starch (MS) was obtained. The final product was also dried under the same conditions. The modification reaction mechanism of the native starch is given in Scheme 1.

2.3. Characterization

Both native (S) and modified starches (MS) were subjected to the following characterizations before ER measurements to be carried out:

The particles of S and MS were mixed with dried KBr and then turned into pellets for FT-IR analysis (Mattson Model 1000 instrument, UK).

Thermal analysis data of particles were obtained using a Setaram 8ET8 V8 Evolution 1760 model thermogravimetric analyzer (TGA) in the presence of nitrogen atmosphere up to 600 °C, at a heating rate of 10 °C/min.

The ^{1}H and ^{13}C NMR spectra were obtained in DMSO-d_6 and $CDCl_3$ at ambient temperature using a 400 MHz Bruker DPX Avonce NMR Spectrometer at the Ankara Test and Analysis Laboratory (ATAL) of Scientific and Technical Research Council of Turkey (TUBITAK).

The energy positions of O and C in S and MS were determined by X-ray energy dispersion analysis (EDS). These samples were scanned by scanning electron microscope (SEM) with an extra of EDS analyzer (Jeol JSM-6360 LV, Japan).

Particle sizes of the samples were determined using a Malvern Mastersizer E, version 1.2b particle size analyzer (UK). The particle sizes for S and MS were determined via Fraunhofer diffraction theory by the Malvern Software computer as 16.26 and 19.29 µm, respectively.

Conductivity measurements were carried out using a Four-Probe technique.

2.4. Preparation of suspensions

Suspensions of S and MS particles were prepared in corn oil at a series of concentration (*c* = 5–40%, m/m), by dispersing definite amount of dispersed phase in calculated amount of continuous phase according to formula:

$$(\mathrm{m/m},\ \%) = \frac{m_{\text{dispersed phase}}}{m_{\text{dispersed phase}} + m_{\text{oil}}} \times 100 \qquad (1)$$

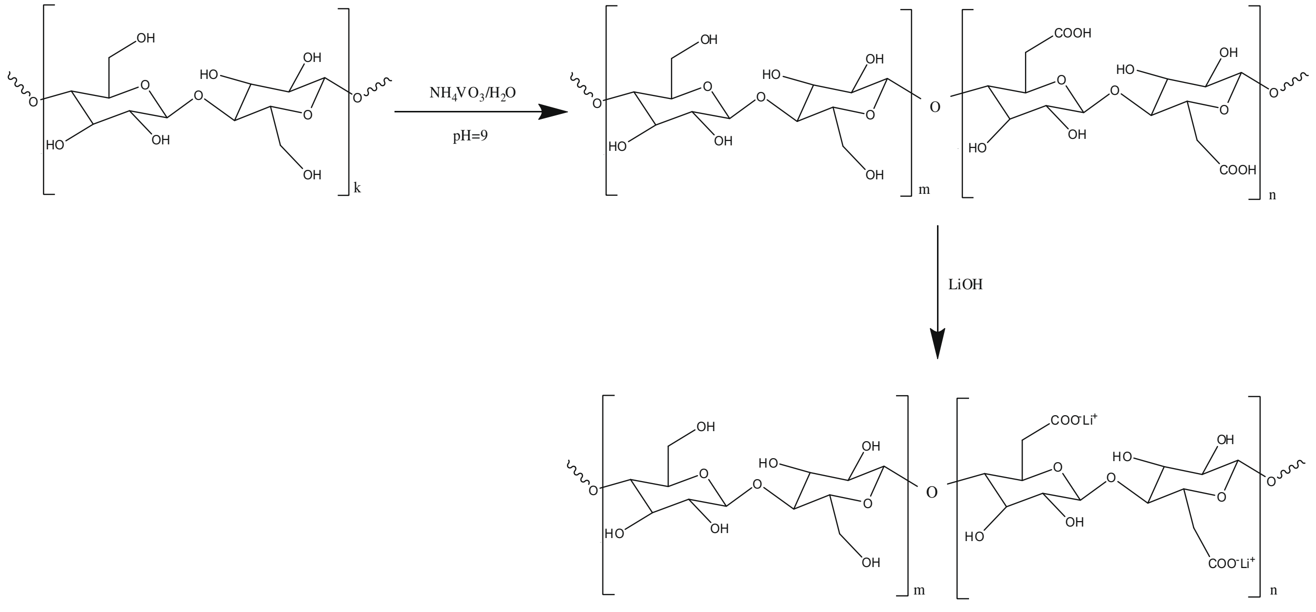

Scheme 1. The modification reaction mechanism of native starch. [$k = (m + n)$; m = % 92.5 n = % 7.5 from NMR data].

2.5. The Electrorheological measurements

The ER fluids were prepared by dispersing S and MS particles in CO. Concentration of these fluids were changed from 5% to 40% (m/m). Rheological properties of the suspension were investigated in a DC field using a Termo-Haake RS600 parallel plate electro-rheometer (Germany). The gap between the parallel plates was 1.0 mm and the diameters of the upper and lower plates were 35 mm. All the experiments were carried out at a controlled rate (CR) mode [except for the shear modulus (G') versus frequency (f) graph, which is carried out at controlled stress (CS) mode] and at various temperatures (25–80 °C, with 5 °C increments.). The voltage used in these experiments was also supplied by a 0–12.5 kV (with 0.5 kV increments) dc electric field generator (Fug Electronics, HCl 14, Germany), which enabled resistivity to be created during the experiments.

3. Results and discussions

3.1. Characterizations

Modified starch was successfully prepared from native starch. In FT-IR spectra of S, the following absorptions were observed: O–H stretching at 3330 cm^{-1}, aliphatic C–H stretching at 2980 cm^{-1}, aliphatic C–H bending at 1460 cm^{-1}, C–H bending at 1170 cm^{-1} and C–O–C symmetric bending at 1025 cm^{-1}. MS was also giver an FT-IR spectrum similar to that of S, with an additional absorption at 1710 cm^{-1} corresponding to C=O stretching, indicating successful conversion of some of the –OH units of native starch to –COOH units (Fig. 1).

^{1}H NMR spectra of S and MS gave the expected distinctive chemical shifts. The signals at 3.35, 3.57, 3.65 and 4.58 ppm were successfully ascribed to the ring protons of H2, H4, H3 and H5, respectively, of the both S and MS. The integral ratio of the new peak appearing at 4.37 ppm of MS shown that the S was successfully partially hydrolyzed at a degree of 7.5%, which was aimed to be 8% for ER purposes.

The native starch gave expected distinctive peaks at ^{13}C NMR. The MS was shown similar ^{13}C spectrum to that of the S. This indicates that the modification did not have an effect on the molecular packing of the double helices in the crystalline regions of S. Beside, the intensity of the peak belonging to C_6 primary –OH group appearing at 59 ppm was gradually decreased and a new peak appeared at 176.12 ppm corresponding to carbonyl carbons in ester groups, which is another proof of the successful modification.

EDS analysis evaluates the extent of ionic types (Mi, Sung, Su, & Peng, 2003). The study of EDS analysis reveals that (Fig. 2) reactions of modification were completed positively. EDS image of S (Fig. 2a) was shown the energy profiles corresponding to O and C atoms present in the molecular structure. On the other hand, EDS image of MS (Fig. 2b) was shown extra Li peak beside O and C atoms, indicating that partially conversion to lithium-salt was successful.

When the TGA curves of S and MS samples were examined (Fig. 3); removal of adsorbed H_2O was detected at 60–110 °C. Two-step degradation temperature (250 °C) was observed to be the same for both S and MS (Vijaya, Popuri, Boddu, & Krishnaiah, 2008). The sum of TGA data for the both samples is tabulated in Table 1. The first degradation peaks corresponds to the removal of ions present in the structure. However, the maximum temperature of degradation of MS (268 °C) was lower than that of S (350 °C). The second degradation peaks corresponds to the degradation of polymeric chains of S. Second decomposition temperature of S is bigger than that of MS. MS leaves more residue than S (12%), which is an indication of more thermal stability for MS. This is due to the high bonding energy of carbonyl group. From TGA analysis, it was concluded that, MS is thermally more stable than S.

3.2. Electrorheology

3.2.1. Sedimentation stability

Despite the recent activities surrounding ER fluids and ER effect, little efforts have focused on the colloidal stability of these suspensions. When the density of particles is not the same as that of medium, the particles with micron size settle down according to Stoke's law (Uemura, Minagava, Takimato, & Koyama, 1995). In order to solve the traditional problem of particle sedimentation, several workers have developed different solutions (Rejon, Ramirez, Paz, Goycoolea, & Valdez, 2002). S/CO and MS/CO suspensions exhibited the same amount of colloidal stability against sedimentation, with

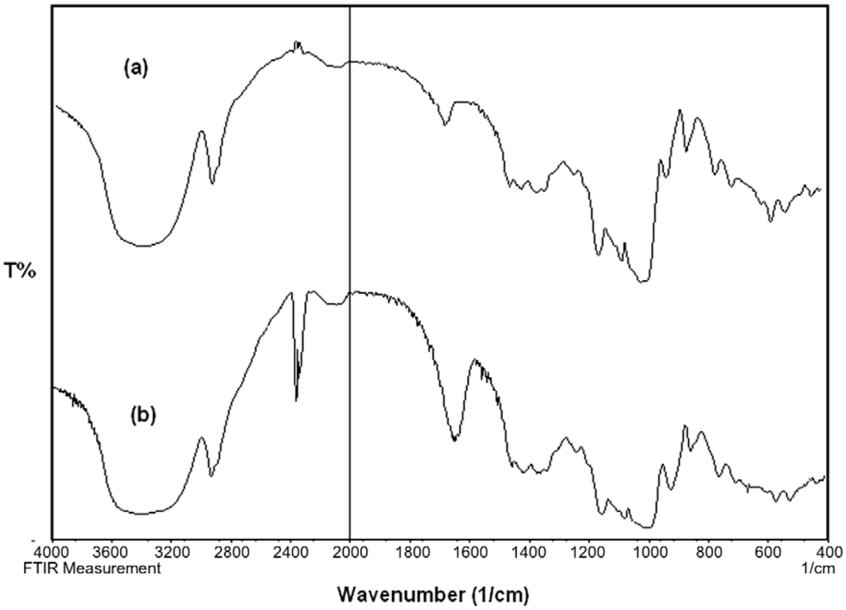

Fig. 1. FT-IR spectra of (a) starch (b) modified starch.

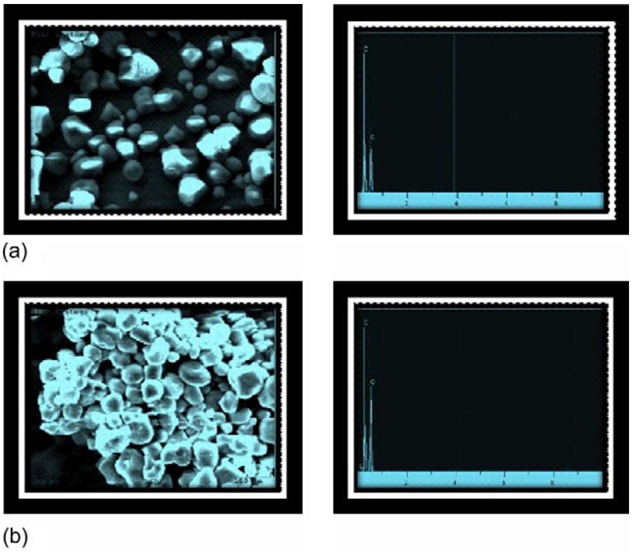
(a)

(b)

Fig. 2. EDS analysis of energy positions (a) starch (b) modified starch.

the sedimentation ratio of 56% at the end of 30 days. This may be attributed to the small hydrolysis ratio of the S.

Table 1
TGA analysis results of starch and modified starch.

Sample	T_i (°C)	T_{max} (°C)	T_f (°C)	600 °C residue (%)
Starch	250	350	450	0
	450	483	515	
Modified starch	250	268	285	12
	400	468	535	

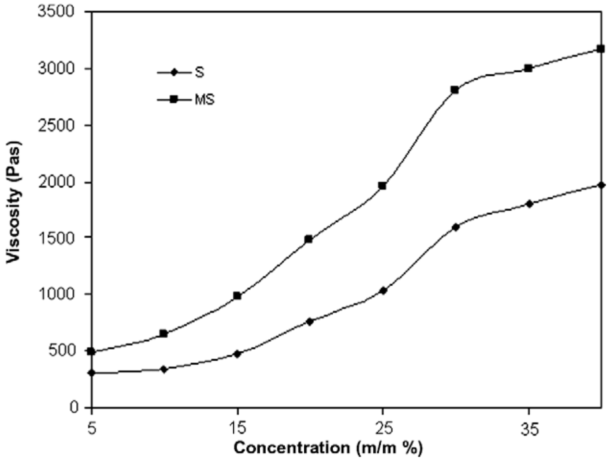

Fig. 4. The change in viscosity with concentration, $T = 20$ °C and $E = 2$ kV/mm.

3.2.2. Effect of dispersed particle concentration

Effect of dispersed particle concentration on viscosity of S/CO and MS/CO suspensions was investigated using five different concentrations (5–40%) and results obtained are shown in Fig. 4. Suspension concentration exerts principle effect on the ER activity. The viscosities of both S and MS were shown increase with rising particle concentration up to $c = 30$ (%, m/m) and then leveled off. The maximum electric field induced viscosities (η_E) of S and MS were observed to be 1976 and 3170 Pa s, respectively under $E = 2$ kV/mm and shown a typical strong ER effect. The increase in ER activity may be attributed to the polarization forces acting between suspended particles of S and MS. In dilute suspensions, according to the Lennard-Johns potential energy diagram, due to the large distance between dispersed particles, the magnitude of this polarization force (F) in the direction of the applied electric field (E) decreases according to the formula (Wu & Shen, 1996):

$$F = 6\varepsilon_2 r^6 E^2 / \varepsilon^4 \tag{2}$$

where ε_2 is the dielectric constant of the particle, ρ is the distance between particles, and r is the radius of the particle.

The effect of particle concentration of polyaniline/silicone oil suspensions was investigated by Lengalova and co-workers (Lengalova et al., 2003) using suspensions of varying concentrations from 5% to 25% at 20, 40 and 60 °C. The η_E of the suspensions in all three temperatures was reported to increase up to 15% concentration and then leveled off.

3.2.3. Effect of electric field strength

An ER fluid forms chain-like structure under a high E, and electrostatic forces become active due to polarization of particles. At

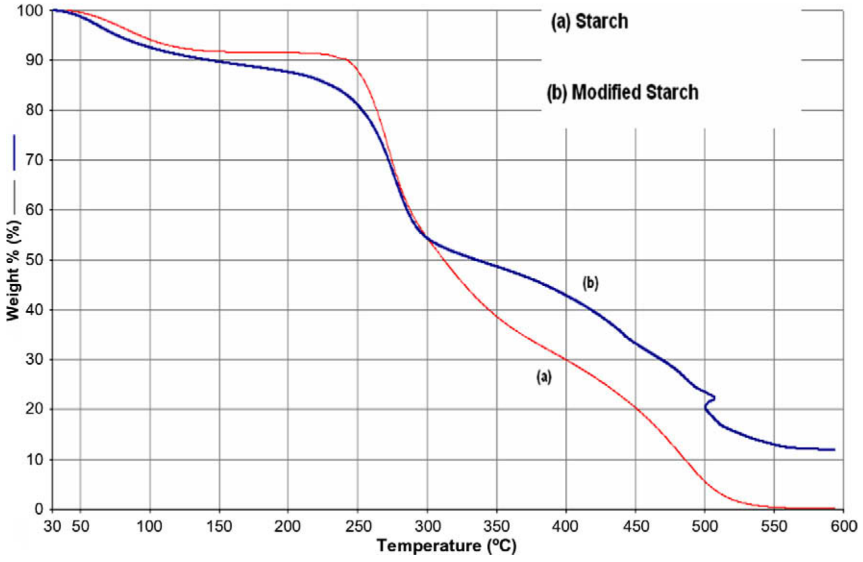

Fig. 3. TGA of (a) starch (b) modified starch.

the same time, also other forces begin to occur in the ER fluid such as: hydrodynamic forces of particles in mobile phase, Brownian motions (providing thermal mobility in suspensions), instantaneous electrostatic repulsive forces or steric interactions, adhesive forces of water or surfactant, van der Waals attractive and electrostatic repulsive forces. Structure of ER suspensions and degree of ER activities both depend on the competition between all of these forces (Winslow, 1953).

Effect of electric field strength (E) on viscosity (η_E) for S and MS is examined in Fig. 5. Both for S and MS linear increases in η_E were observed. The maximum η_E values for S and MS were determined to be 2.4 and 6.0 kPa s, respectively, which correspond to 2.5 times increase in η_E in MS after Li-salt formation. Under applied E, the magnitude of the polarization forces between particles increases, and in turn, the particles rapidly aggregate into the chain formation perpendicular to the electrodes, hence resulting in improvement of the η_E.

Choi and co-workers stated that the viscosity of polyaniline/silicon oil suspensions increases with increasing E linearly (Choi, Kim, Cho, Kim, & Jhon, 1997). Similar trend was reported for the study of $CaCO_3$/silicon oil system by Yilmaz and co-workers (Yilmaz, Unal, & Yavuz, 2005).

Shear stress is one of the critical design parameter in ER phenomenon and has attracted considerable attention both theoretically and experimentally. Fig. 5 also shows the changes in the shear stress (τ) of S/CO and MS/CO suspensions under various E values. Increase in E causes increase in τ. This is due to the formation of chain-like structure caused by the polarized particles in suspensions under E (Choi, Park, & Lee, 2002).

Although a linear change of τ with E^2 is reported in the literature by some researchers (Conrad & Chen, 1970), such a behavior was not observed for both S/CO and MS/CO suspensions. Similar behavior to S/CO and MS/CO suspensions was also reported for other suspension systems including potato starch phosphate (Park et al., 2004) and cyclodextrin–epichlorohydrin–starch polymer suspensions (Gao & Zhao, 2004).

3.2.4. Effect of shear rate on viscosity and shear stress

Change in the viscosity of S/CO and MS/CO suspensions with shear rate ($\dot{\gamma}$) is shown in Fig. 6. As is evident, the viscosity of S/CO and MS/CO suspensions decreases sharply with increasing $\dot{\gamma}$ and giving a typical curve of shear thinning non-Newtonian viscoelastic behavior under $E = 0$ and $E = 2$ kV/mm conditions (Ling & Keqin, 2006; Lengalova et al., 2003).

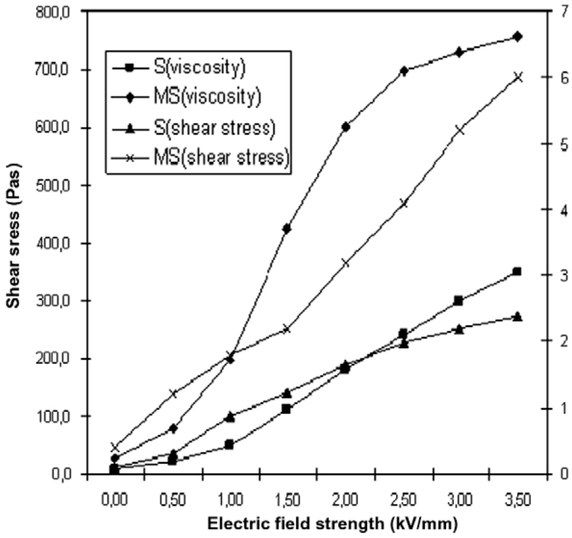

Fig. 5. The change of viscosity and shear stress with electric field strength, $T = 20$ °C, $c = 30\%$ m/m, $\dot{\gamma} = 0.2\ s^{-1}$.

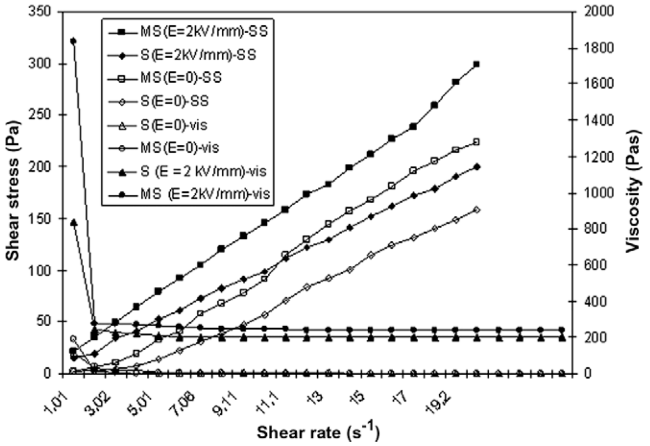

Fig. 6. The change of viscosity and shear stress with shear rate, $T = 20$ °C, $c = 30\%$ m/m, $E = 0$ and 2 kV/mm.

Change of τ with $\dot{\gamma}$ is also shown in Fig. 6. Shear stress of S/CO and MS/CO suspensions observed to increase with increasing $\dot{\gamma}$ between $\dot{\gamma} = 0.01–20.0\ s^{-1}$; and the τ values of S increased from 158 Pa ($E = 0$ kV/mm) to 200 Pa ($E = 2.0$ kV/mm) and τ values of MS increased from 224 Pa ($E = 0$ kV/mm) to 300 Pa ($E = 2.0$ kV/mm). Effect of E on τ for the both materials is clearly seen. Both S and MS were shown a Newtonian flow behavior in the absence of E ($E = 0$ kV/mm). But, Bingham plastic behavior was observed under $E = 2$ kV/mm condition with yield stresses (τ_y) of 15 and 22 Pa for S and MS, respectively. This is caused by the role of electric field induced polarization forces, which is a typical rheological characteristic of ER fluids under the influence of external E (Ko, Sung, & Choi, 2007).

3.2.5. Effect of temperature

The temperature dependence of the shear stress is shown in Fig. 7. The results were investigated at temperatures between 25 and 80 °C. It was observed that, for S/CO system, τ decreased with increasing T and a shear stress loss of $\Delta\tau = 118$ Pa was measured.

An interesting curve was obtained for MS/CO suspension, showing a decrease in τ up to $T = 50$ °C, then gave an increase with rising T. This may be attributed to the loss of moisture in the MS/CO suspension and the increased kinetic energy of Li^+ ions inserted into the structure of S with the modification process, which gave rise to increased mobility and polarizability of the suspended starch–Li particles.

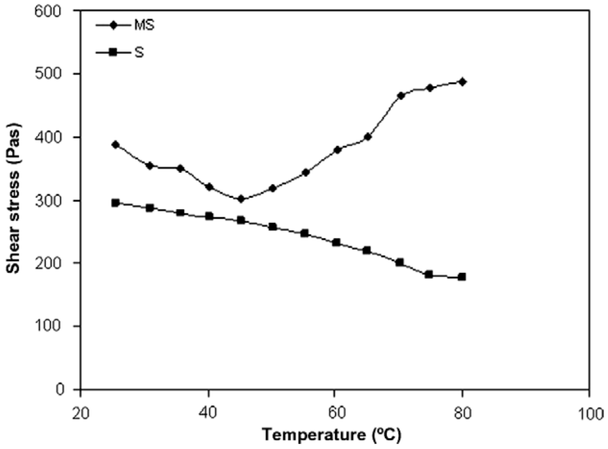

Fig. 7. Effect of temperature on the shear stress for starch and modified starch suspension, $c = 30\%$ m/m, $\dot{\gamma} = 0.2\ s^{-1}$, $E = 2.0$ kV/mm.

Generally, the temperature has two effects on the ER fluids: one is on the polarization forces and the other is on the Brownian motion. The increase of temperature results both in activation energy decrease of polarization of suspended particles, and on the polarizability of particles; which results in a decrease in shear stress. On the other hand, the Brownian motion does not contribute to chain formation of suspended particles. Both shear stress increases (Lu & Zhao, 2002) and shear stress decreases (Unal et al., 2006) and (Liu & Shaw, 2001) were reported in the literature, depending on the ER system studied.

3.2.6. Effect of frequency

The effect of frequency (*f*) on the shear modulus (*G*′) for S/CO and MS/CO suspension is shown Fig. 8. Up to *f* = 50 Hz, viscoelastic properties of both S and MS were not much changed. After *f* = 50 Hz, a sharp increase was observed for each sample as a typical characteristic of a viscoelastic material, which indicates a vibration damping property. The increase in *G*′ with increasing external *f* was also reported in the literature (Hiamtup, Sirivat, & Jameison, 2006; Kim et al., 2001).

3.2.7. The creep behavior

During the creep experiment, a constant stress ($\tau = 10$ Pa) was applied instantaneously (for 10 s) to S/CO and MS/CO suspensions at constant conditions and change in the strain (γ) was measured over a period of time (Fig. 9). It was observed that γ increases continuously with time; and when the applied stress was removed, the time-dependent deformation was recovered. The creep curve comprises three parts: the instantaneous strain, the retardation strain, and the viscous strain. Also, the samples show an instantaneous elastic recovery, followed by a recovery process when the applied stress is removed. It is apparent that at this stress level, the sample is in non-linear viscoelastic regime. The suspensions were instantaneously deformed under applied stress and then, this strain was recovered after the removal of the stress. The energy used for chain stretching is stored. On the other hand, non-linear viscoelastic recovery was obtained for both S/CO and MS/CO systems when the applied stress was removed. For the materials studied in this work, % recoverable strain data are 53.97% and 72.4% for S/CO and MS/CO, respectively which was calculated from the relation (Cho et al., 2004),

$$\%\text{recoverable strain} = \frac{\gamma_i - \gamma_f}{\gamma_i} \times 100 \tag{3}$$

where γ_i is the total strain acquired before removing the applied stress and γ_f is the average steady state strain after removing the applied stress. As expected, % recoverable strain of MS was bigger than S. The increase of recoverable strain from 53.97% (S/CO) to 72.4% (MS/CO) indicates that, after modification S became more ER active under *E*.

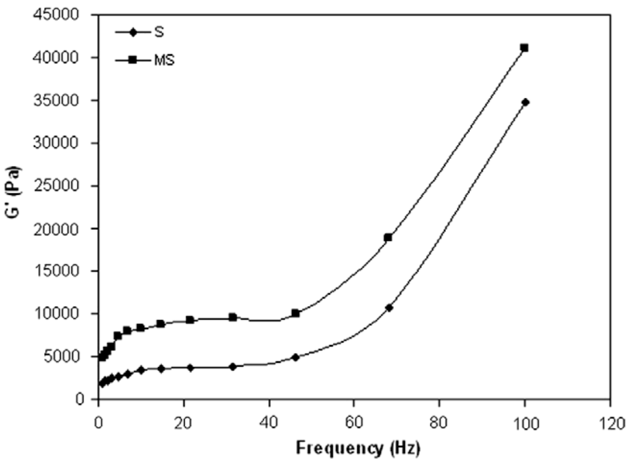

Fig. 8. The change of *G*′ with frequency, *c* = 30% m/m, *T* = 20 °C, γ = 10 Pa, *E* = 2 kV/mm.

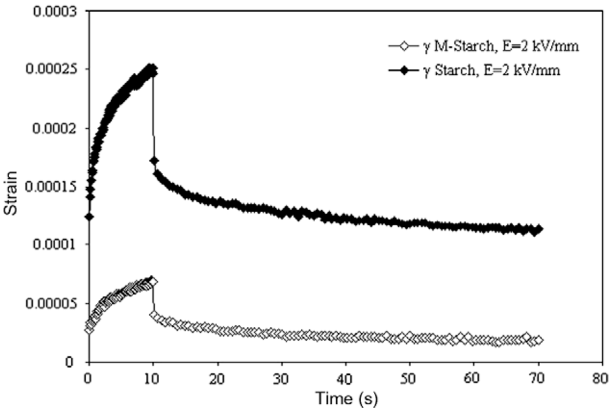

Fig. 9. Creep behavior of S and MS. *T* = 20 °C, *c* = 30% m/m, *E* = 2 kV/mm.

4. Conclusions

In present study we have shown that the native starch can successfully be partially modified and converted to ER active Li-salt.

The results shown that, S/CO and MS/CO suspensions exhibited ER behavior under electric field strength. The conductivities of S (10^{-9} S/m) and MS (10^{-5} S/m) were in the range of ER active materials. Sedimentation stabilities of S/CO and MS/CO suspensions were found to be 56% and suitable for potential industrial applications. Optimum particle concentration of the both suspensions was determined to be 30% by mass. The shear stresses of the both materials were shown a linear increase with increasing *E*. S/CO and MS/CO suspensions showed Newtonian behavior when $E = 0$ kV and Bingham behavior when $E \neq 0$ kV. The viscosities of S/CO and MS/CO suspensions decreased with increasing shear rate and given a typical of viscoelastic behavior by means of shear thinning. Electric field induced viscosities of the both materials were observed to increase linearly. Temperature was observed to be effective on the both materials and caused shear stress losses on S and shear stress increase on MS, especially at elevated temperatures. Our results revealed that, wet-base ER active S/CO suspension system become dry-base ER active after the modification, and shown 3 times stronger ER strength; which is extremely important from industrial point of view.

Acknowledgement

The authors thanks to TUBITAK (The Scientific and Technical Research Council of Turkey) for the financial support of this work (Project No: 107T628).

References

An, Y., Liu, B., & Shaw, M. T. (2002). Soft gels with ordered iron particles: Fabrication and electrorheological response. *International Journal of Modern Physics B, 16*, 2440–2446.

Cho, M. S., Lee, J. H., Choi, H. J., Ahn, K. H., Lee, S. J., & Jeon, D. (2004). Linear viscoelasticity of semiconducting polyaniline based electrorheological suspensions. *Journal of Materials Science, 39*, 1377–1382.

Choi, H. J., Kim, T. W., Cho, M. S., Kim, S. G., & Jhon, M. S. (1997). Electrorheological characterization of polyaniline dispersions. *European Polymer Journal, 33*, 699–703.

Choi, U., Park, Y., & Lee, S. (2002). Electrorheological behavior of chitosan succinate suspension as an anhydrous ER fluid. *Journal of Colloids & Surfaces, 211*, 85–90.

Conrad, H., & Chen, Y. (1970). *Progress in electrorheology*. New York: Plenum Press. p. 55.

Gao, Z., & Zhao, X. (2004). Preparation and electrorheological characteristics of β-cyclodextrin–epichlorohydrin–starch polymer suspensions. *Journal of Applied Polymer Science, 93*, 1681–1686.

Gonon, P., Foulc, J. N., & Atten, P. (2001). A conduction model describing particle–particle interaction in the case of surface conducting particles. *International Journal of Modern Physics B, 15*, 704–713.

Hao, T., Xu, Z., & Xu, Y. J. (1997). Correlation of the dielectric properties of dispersed particles with the electrorheological effect. *Journal of Colloid & Interface Science, 190*, 334–340.

Hiamtup, P., Sirivat, A., & Jameison, A. M. (2006). Electrorheological properties of polyaniline suspensions: Field-induced liquid to solid transition and residual gel structure. *Journal of Colloid & Interface Science, 295*, 270–278.

Hong, C. H., Sung, J. H., & Choi, H. J. (2009). Effects of medium oil on electroresponsive characteristics of chitosan suspensions. *Colloid Polymer Science, 287*, 583–589.

Kim, J. W., Cho, Y. H., Choi, H. J., Lee, H. G., & Choi, S. B. (2002). Electrorheological semi-active damper: Polyaniline based ER system. *Journal of Intelligent Material Systems & Structures, 13*(7–8), 509–513.

Kim, J. W., Choi, H. J., & Jhon, M. S. (2000). Synthesis and electrorheological characterization of emulsion polymerized SAN-clay nanocomposite suspensions. *Macromolecular Symposia, 155*, 229–237.

Kim, S. G., Kim, J. W., Jang, W. H., Choi, H. J., & Jhon, M. S. (2001). Electrorheological characteristics of phosphate cellulose-based suspensions. *Polymer, 42*(11), 5005–5012.

Kim, J. W., Noh, M. H., Choi, H. J., Lee, D. C., & Jhon, M. S. (2000). Synthesis and electrorheological characteristics of SAN-clay composite suspensions. *Polymer, 41*, 1229–1231.

Ko, Y. G., Sung, B. H., & Choi, U. S. (2007). Electrorheological properties of aminated chitosans. *Colloids and Surfaces. A Physicochemical & Engineering Aspects, 305*, 120–125.

Lengalova, A., Pavlinek, V., Saha, P., Quadrat, O., Kitano, T., & Stejskal, J. (2003). Influence of particle concentration on the electrorheological efficiency of polyaniline suspensions. *European Polymer Journal, 39*, 641–645.

Ling, R., & Keqin, Z. (2006). Electrorheological effects at high shear rate. *Tsinghua Science & Technology, 11*(1), 88–95.

Liu, B., & Shaw, M. T. (2001). Electrorheology of filled silicone elastomers. *Journal of Rheology, 45*, 641–657.

Lu, J., & Zhao, X. (2002). Electrorheological behaviors of polyaniline-montmorillonite clay nanocomposite. *International Modern Physics B, 16*(17–18), 2521–2527.

Mi, F. L., Sung, H. W., Su, C. C., & Peng, C. K. (2003). Synthesis and characterization of biodegradable TPP/genipin co-crosslinked chitosan gel beads. *Polymer, 44*, 6521–6530.

Ogungbenle, H. (2007). Effect of chemical modification on starch of some legume flours. *Pakistan Journal of Nutrition, 6*(2), 167–171.

Okamura, H., Suzuki, K., Mori, T., Minagawa, K., Masuda, S., & Tanaka, M. (2002). Chain behavior in model homogeneous ER fluids depending on temperature. *International Modern Physics B, 16*(17–18), 2385–2391.

Park, D. P., Sung, J. H., Kim, C. A., Choi, H. J., & Jhon, M. S. (2004). Synthesis and electrorheology of potato starch phosphate. *Journal of Applied Polymer Science, 91*, 1770–1773.

Parthasarathy, M., & Klingenberg, D. J. (1996). Electrorheology: Mechanisms and models. *Materials Science & Engineering, R17*, 57–103.

Rejon, L. A., Ramirez, F., Paz, F. M., Goycoolea, F. M., & Valdez, M. A. (2002). Response time and electrorheology of semidiluted gellan, xanthan and cellulose suspension. *Carbohydrate Polymers, 48*, 413–421.

Shimada, K., Nishida, H., & Fujita, T. (2001). Differences in steady characteristics and response time of ERF on rotational flow between rotating disk and concentric cylinder. *International Journal of Modern Physics B, 15*, 1050–1056.

Uemura, T., Minagava, K., Takimato, J., & Koyama, K. (1995). Opposite Electrorheological effects between urethane-based polymers having different terminal groups. *Journal of Chemical Society Faraday Transactions, 91*(6), 1051–1052.

Unal, H. I., Agirbas, O., & Yilmaz, H. (2006). Electrorheological properties of poly(Li-2-hydroxyethyl methacrylate) suspensions. *Colloids and Surfaces. A Physicochemical & Engineering, Aspects, 274*, 77.

Vijaya, Y., Popuri, S. R., Boddu, V. M., & Krishnaiah, A. (2008). Modified chitosan and calcium alginate biopolymer sorbents for removal of nickel (II) through adsorption. *Carbohydrate Polymers, 72*(2), 261–271.

Winslow, W. M., (1953). Field controlled hydraulic device. US Pat. No. 2661596.

Wu, S. Z., & Shen, J. R. (1996). Electrorheological properties of chitin suspensions. *Journal of Applied Polymer Science, 60*(12), 2159–2164.

Yilmaz, H., Unal, H. I., & Yavuz, M. (2005). An investigation of electrorheological properties of calcium carbonate suspensions. *Colloid Journal, 67*(2), 268–273.